Statistical cycling in coupled map lattices

Jérôme Losson
Center for Nonlinear Dynamics and Department of Physics, 3655 Drummond, Room 1125, Montréal, Québec, Canada H3G 1Y6

Michael C. Mackey
Center for Nonlinear Dynamics and Departments of Physics and Physiology, 3655 Drummond, Room 1124, Montréal, Québec, Canada H3G 1Y6

(Received 18 January 1994; revised manuscript received 29 April 1994)

This work describes a class of phase transitions observed in large coupled map lattices (CML's) with chaotic local maps. The phase transitions are seen to occur (1) when the coupling is fixed as other parameters are changed and (2) when the coupling is changed with other parameters fixed. The different phases of the lattices of tent and quadratic maps are interpreted as reflecting different spectral properties of the Perron-Frobenius operator for the CML's. The spectral characteristics of this operator induced by piecewise linear CML's are investigated analytically using general results from the theory of linear operators. Sufficient conditions for the cyclical evolution of phase space densities are given. This implies that the CML's under consideration can reach equilibrium states in which ensemble statistics are not time independent (stationary), but time periodic.

PACS number(s): 05.45.+b, 02.50.−r, 05.70.Ln, 64.60.Cn

I. INTRODUCTION

In this paper we consider a class of phase transitions observed in lattices of coupled one dimensional maps [coupled map lattices (CML's)], which are characterized by the discontinuous behavior of the statistical quantifiers of the activity of the lattice (spatial and temporal correlation functions, the Boltzmann-Gibbs entropy, etc.) as control parameters are varied. Above a critical parameter value (the temperaturelike parameter is the inverse of the coupling between the elements) the system is symmetric under spatial translations and correlation functions decay to zero exponentially fast; in fact, numerical evidence suggests that it is spatiotemporally chaotic in the usual sense [1–3] and therefore mixing. Below the critical point, the system loses this symmetry and can spontaneously form very large scale patterns for all coupling strengths. These qualitative changes in the behavior of the CML's are reminiscent of phase transitions described in classical statistical mechanics, rather than bifurcations in the traditional sense of the term [4], because they correspond to changes of the thermodynamic state of the lattice and are inherently "probabilistic" (this is discussed further in Sec. II). Similar transitions have been recently numerically characterized by Miller and Huse in an odd piecewise linear map CML with constant coupling [5] and are described by these authors as *paramagnetic-ferromagnetic* transitions. However, these transitions have not yet been shown analytically to reflect the nonanalytic behavior of a function playing the role of the free energy for the CML (namely, the topological pressure; cf. [6] and Remark 2 of Sec. II below) and therefore a rigorous analogy with statistical mechanics remains somewhat premature at this point.

Here the phase transitions are explained in terms of abrupt changes of the spectral properties of the Perron-Frobenius (PF) operator induced by the CML. Above the transition, this operator is asymptotically stable, a dynamical property which implies mixing. Below the transition, the PF operator displays asymptotic periodicity, a dynamical property which implies that the thermodynamic equilibrium for the lattice consists in a sequence of metastable states visited periodically in time. This type of cyclical behavior has been reported in various cellular automata and in certain CML's by Chaté and Manneville [7], Gallas *et al.* [8], and Kaneko [9], and commented on by Pomeau (cf. [10] and references therein). The discussion of the PF operator for the CML's undergoing the phase transitions allows one to describe both the equilibrium and the far-from-equilibrium states using the same conceptual framework, which involves looking at the spectral properties of a linear Markov operator governing the evolution of absolutely continuous measures (or their densities).

In Sec. II we motivate the study of the evolution of phase space densities for coupled map lattices as a means to study the nonequilibrium thermodynamics of these systems; the Perron-Frobenius operator is introduced. In Sec. III the dynamics of CML's with diffusive coupling and piecewise linear as well as quadratic local nonlinearities are explored numerically. Statistical quantifiers of the motion are introduced and their behavior is used to characterize the two "phases" of the CML. Spectral properties of the Perron-Frobenius operator in higher dimensions are discussed in Sec. IV. In Sec. V these spectral properties are examined analytically in lattices of diffusively coupled tent maps. We give sufficient conditions for the Perron-Frobenius operator for these CML's to be asymptotically periodic and examine the numerical results of Sec. II in light of these conditions.

Background on CML's

The systems we study here are arbitrarily large but finite and of the form

$$x_{t+1}^{i}=(1-\varepsilon)S(x_t^i)+\frac{\varepsilon}{p}\sum_{\substack{j\\ p\text{ neighbors}}} S(x_t^j)\ , \tag{1}$$

where S: $[0,1]\mapsto[0,1]$ is the local map and $\varepsilon\in[0,1]$ is the coupling term; i denotes a discrete space index (of arbitrary finite dimension) and t denotes discrete time. As an interesting special case, we focus on the nearest neighbor coupling case on a two-dimensional $L\times M$ lattice with periodic boundary conditions:

$$\begin{aligned}x_{t+1}^{i,j}=&(1-\varepsilon)S(x_t^{i,j})+\frac{\varepsilon}{4}[S(x_t^{i-1,j})\\&+S(x_t^{i+1,j})+S(x_t^{i,j-1})+S(x_t^{i,j+1})]\\&i=1,\ldots,L;\quad j=1,\ldots,M;\quad t\in\mathbb{R}^+\ .\end{aligned} \tag{2}$$

The nearest neighbor coupling on a body centered cubic lattice is a discrete-space version of the diffusion operator [11]. A series of papers dealing with various motivations for studying CML's such as (1) and (2) can be found in the references of [12].

There are important analytical results by Keller and Künzle [2], Bunimovich and Sinai [1], and Gundlach and Rand [3] related to the construction of equilibrium statistical mechanics for systems close to (1) (except for [1] in which the coupling is somewhat different). The main questions addressed by these authors are the existence and uniqueness of absolutely continuous invariant measures for the spatiotemporal (semi)dynamical systems associated with the CML. The investigations follow two broad (and intersecting) paths. One involves mapping the CML to a lattice spin system via the introduction of symbolic dynamics and then considering the evolution of the CML using the theory of Gibbs random fields. This is the approach of Bunimovich and Sinai, and Rand and Gundlach, and it is essentially an extension of the so-called thermodynamic formalism [13] of Ruelle, Bowen, Sinai, and others to infinite-dimensional hyperbolic dynamical systems. The other involves the study of the Perron-Frobenius operator for CML's (defined in Sec. II). This is the approach of Keller and Künzle [2], which yields results similar to those of [1,14] in the case of infinite-dimensional lattices, with more general coupling schemes, but somewhat more restrictive expansion conditions. For finite-dimensional lattices, they describe the spectral decomposition of the PF operator for a CML, but the conditions they give for the applicability of their results involve lengthly calculations. Here we use results of Góra and Boyarski [15] to demonstrate that asymptotic periodicity of the Perron-Frobenius operator is a property which permits a rigorous mathematical description of the thermodynamic equilibrium of CML's discussed in the literature [7,16,12] and which display "statistical cycling."

II. THE EVOLUTION OF ENSEMBLE DENSITIES FOR CML'S

Statistical quantifiers of CML dynamics are computed, like their counterparts in classical statistical mechanics, with respect to some ensemble density. At equilibrium, this density can be derived for some systems [e.g., the Boltzmann density for the Ising model at a finite temperature, the invariant density $f(x)=1/\pi\sqrt{x(1-x)}$ for the quadratic map when $r=4$, etc.]. Formally, the thermodynamic state of a (semi)dynamical system Φ: $\mathbb{X}\mapsto\mathbb{X}$ is the measure space $(\mathbb{X},\mathcal{B},\mu_t)$, where $\mathcal{B}$ is a finite σ algebra and μ_t is a measure defined on $\mathcal{B}$ at time t. In the cases which concern us here, the measure μ_t is absolutely continuous with respect to the Lebesgue measure and therefore is associated with a density function $f_t(x)$ by the relation $\mu_t(A)=\int_A f_t(x)dx$ for all $A\in\mathcal{B}$. As time evolves, the phase space $\mathbb{X}$ and $\mathcal{B}$ (which is a partition of $\mathbb{X}$) remain the same, so that the evolution of the thermodynamic state of Φ is described by the evolution of the phase space densities $f_t(x)$ associated with the measures μ_t. The state of thermodynamic equilibrium for a nonsingular CML Φ is therefore described by the fixed point f^* of the operator $\mathcal{P}_\Phi$ governing density evolution, when such a fixed point exists (i.e., when there exists f^* such that $\mathcal{P}_\Phi f^*=f^*$). Nonsingular means in this case that $\mu_{\mathbb{X}}^L(\Phi^{-1}(\cdot))$ is absolutely continuous with respect to the Lebesgue measure $\mu_{\mathbb{X}}^L$ on $\mathbb{X}$. Here we study situations where the fixed point exists, but is almost never reached. Instead, the densities almost always evolve to a cycle, and this results in the cycling and time-periodic behavior of statistical quantifiers. If the (semi)dynamical system is associated with a nonsingular CML, then the density evolution operator is the Perron-Frobenius operator.

The Perron-Frobenius operator $\mathcal{P}_\Phi$: $D\mapsto D$ (D, the space of densities, is defined in Sec. IV A) is induced by a measurable transformation Φ: $\mathbb{X}\mapsto\mathbb{X}$, which is nonsingular. For any $f_t\in D$, the Perron-Frobenius operator is defined by

$$\int_A \mathcal{P}_\Phi f_t dx=\int_{\Phi^{-1}(A)} f_t dx\ , \tag{3}$$

where $A\subset\mathbb{X}$. An equivalent definition is also useful in practical examples since it applies to piecewise monotonic transformations. Let $\Phi_i\equiv\Phi_{|A_i}$, where the $A_i\subset\mathbb{X}$, $i=1,\ldots,m$, are the sets over which Φ is monotonic, and $\cup_i A_i=\mathbb{X}$. If Φ is nonsingular, the corresponding Perron-Frobenius operator is defined by

$$f_{t+1}(x)=\mathcal{P}_\Phi f_t(x)=\sum_{i=1}^{m}\frac{f_t(\Phi_i^{-1}(x))}{\det\mathcal{J}(\Phi_i^{-1}(x))}\chi_{\Phi_i(A_i)}(x)\ , \tag{4}$$

where $\chi_{\Phi_i(A_i)}(x)\equiv 1$ if and only if $x\in\Phi_i(A_i)$ and 0 otherwise, and $\det\mathcal{J}(Z)$ is the absolute value of the Jacobian of Z. A more intuitive version of (4) is

$$\mathcal{P}_\Phi f_t(x)=\sum_{y\in\Phi^{-1}(x)}\frac{f_t(y)}{\det\mathcal{J}(\Phi(y))}\ .$$

The operator $\mathcal{P}_\Phi$ is called asymptotically periodic (AP) if there exist finitely many distinct functions

$g_1,\ldots,g_r\in L^1_+$ with disjoint supports [i.e., $g_i(x)g_j(x)=0$ for all x if $i\neq j$; cf. [17] for details], a permutation α of the set $\{1,\ldots,r\}$, and positive continuous linear functionals $\Gamma_1,\ldots,\Gamma_r$ on L^1_+ such that

$$\lim_{n\to\infty}\left|\left|\mathcal{P}_\Phi^n\left[f_0-\sum_{i=1}^{r}\Gamma_i[f_0]g_i\right]\right|\right|_{L^1}=0 \tag{5}$$

and

$$\mathcal{P}_\Phi g_i=g_{\alpha(i)}\ ,\quad i=1,\ldots,r\ .$$

If $\mathcal{P}_\Phi$ satisfies these conditions with $r=1$, it is said to be asymptotically stable, a property which implies mixing and the exponential decay of correlations.

Remark 1. The phase space density f_t of an AP system at any (large) time t is a linear combination of "basis states" (denoted g_i above) with disjoint supports, and at every time step the coefficients (Γ_i) of this linear combination are permuted by α. Therefore, the density evolution in such systems is periodic, with a period bounded by $r!$, but with the exact cycle depending on the initial preparation since the Γ_i's are functionals of the initial density [cf. (5)]. A direct consequence of asymptotic periodicity is that the thermodynamic equilibrium of the system consists in a sequence of metastable states which are visited periodically. AP systems are ergodic if and only if the permutation α is cyclical. ■

Remark 2. When discussing the thermodynamics of dynamical systems, it is useful to generalize the definition of the Perron-Frobenius operator and introduce the so-called *transfer operator* [13,18]

$$\mathcal{P}_{\Phi,\beta}f_t(x)=\sum_{i=1}^{m}\frac{f_t(\Phi_i^{-1}(x))}{|\det\mathcal{J}(\Phi_i^{-1}(x))|^\beta}\chi_{\Phi_i(A_i)}(x)\ ,\quad \beta>0\ ,$$

which reduces to our previous definition when $\beta=1$. Changing β allows us to determine which of the preimages dominate the transfer of mass from $f_t(x)$ to $f_{t+1}(x)$ (i.e., which *microstates* contribute to the density most). To illustrate the connection with classical statistical mechanics, apply $\mathcal{P}_{\Phi,\beta}$ T times to the uniform initial density $f(x,0)=\chi_X(x)$,

$$\begin{aligned}f_T(x)&=\sum_{y^{(i)}\in\Phi_i^{-T}(x)}[\det\mathcal{J}(\Phi_i^{-N}(y^{(i)}))]^{-\beta}\\&=\sum_{y^{(i)}\in\Phi_i^{-T}(x)}\exp\left[-\beta\sum_{t=0}^{T-1}\ln|\Phi_i'(y^{(i)})|\right]\\&=Z_T^{\text{top}}(\beta)\ ,\end{aligned}$$

where the simplified notation $\det\mathcal{J}(\cdot)\to|\cdot'|$ is used. The sum over the $\Phi_i^{-T}(x)$ is over the Tth preimages of x (which is a sum over i), whereas the sum in the exponent runs over iterates of initial values x_0 [distributed according to $f_0(x_0)$]. $Z_T^{\text{top}}(\beta)$ is known as the *topological partition function* [6], which is instrumental in the definition of meaningful thermodynamic quantities for dynamical systems (such as the topological pressure which plays the role of the free energy for hyperbolic systems since it satisfies a variational principle, much as the free energy does in classical statistical mechanics). The interested reader is referred to the clear discussion of the connection between the generalized Perron-Frobenius operator and the transfer matrix methods of classical statistical mechanics found in [6]. ■

For numerical examples, we focus our attention on system (2) with $S(x)$ given by the generalized tent map

$$S(x)=\begin{cases}ax & \text{if } x\in[0,\frac{1}{2})\\ a(1-x) & \text{if } x\in[\frac{1}{2},1]\end{cases}\quad 1<a\leq 2\ . \tag{6}$$

This CML is interesting because there is strong numerical evidence of asymptotic periodicity in large regions of the (a,ε) plane; in addition, the piecewise linear nature of the CML allows one to explicitly compute the eigenvalues of the absolute value of the derivative transformation and carry out calculations efficiently in Sec. V.

There is also analytical proof that asymptotic periodicity is present in the one-dimensional map [19,20] and in two diffusively coupled maps [21]. The Perron-Frobenius equation (3) for the hat map (6) is

$$\mathcal{P}f(x)=\frac{1}{a}\left[f\left[\frac{x}{a}\right]+f\left[1-\frac{x}{a}\right]\right]\ . \tag{7}$$

This operator was described by Yoshida, Mori, and Shigematsu [20] and Provatas and Mackey [19] and the following results on asymptotic periodicity are available:

$$\begin{aligned}&2^{1/2^{n+1}}<a\leq 2^{1/2^n}\\&\quad\Longleftrightarrow\text{asymptotic periodicity of period-}2^n\ ,\\&\qquad\qquad n=0,1,2,\ldots\end{aligned} \tag{8}$$

A generalization of this result was derived for two diffusively coupled tent maps [21]. The next section gives numerical evidence that period-2^n asymptotic periodicity is also present in large CML's. Before proceeding, we show in Fig. 1 the nature of the density evolution for the hat map when its Perron-Frobenius operator is asymptotically periodic with period-2 and period-4.

The other system that will be considered here is the CML (2) with the local nonlinearity given by the quadratic map

$$S(x)=rx(1-x)\ ,\quad r\in(r_c,4]\ , \tag{9}$$

where $r_c\simeq 3.57\ldots$ is the parameter value at which the transition to chaos occurs beyond the period doubling scenario. The motivation for including the quadratic map in this discussion is that it is shown to display much of the behavior displayed by the simpler tent map, therefore leading us to the conjecture that the phase transitions explored here are to be expected generically in large classes of systems (not necessary everywhere expanding). Again from (3) and using $A=[0,x]$ it is easy to see that the Perron-Frobenius operator for the quadratic map is

$$\mathcal{P}f(x)=\frac{1}{\left[1-\frac{4x}{r}\right]^{1/2}}\left\{f\left[\frac{1}{2}+\frac{1}{2}\left[1-\frac{4x}{r}\right]^{1/2}\right]+f\left[\frac{1}{2}-\frac{1}{2}\left[1-\frac{4x}{r}\right]^{1/2}\right]\right\}. \tag{10}$$

When $r=4$ the Perron-Frobenius operator is asymptotically stable and the density of the invariant measure is

$$f^*(x)=\frac{1}{\pi\sqrt{x(1-x)}}.$$

It was proved by Jakobson [22] that an absolutely continuous invariant measure exists for values of r forming a set of positive Lebesgue measure, although $r=4$ is the only value at which f^* can be given explicitly. There is, in addition, a spectrum of values, labeled r_n, $n=1,2,\ldots$, where so-called banded chaos [23] has been reported numerically. At these values, the iterates of the quadratic map resemble those of the tent map when it is asymptotically periodic: The phase space densities oscillate periodi-

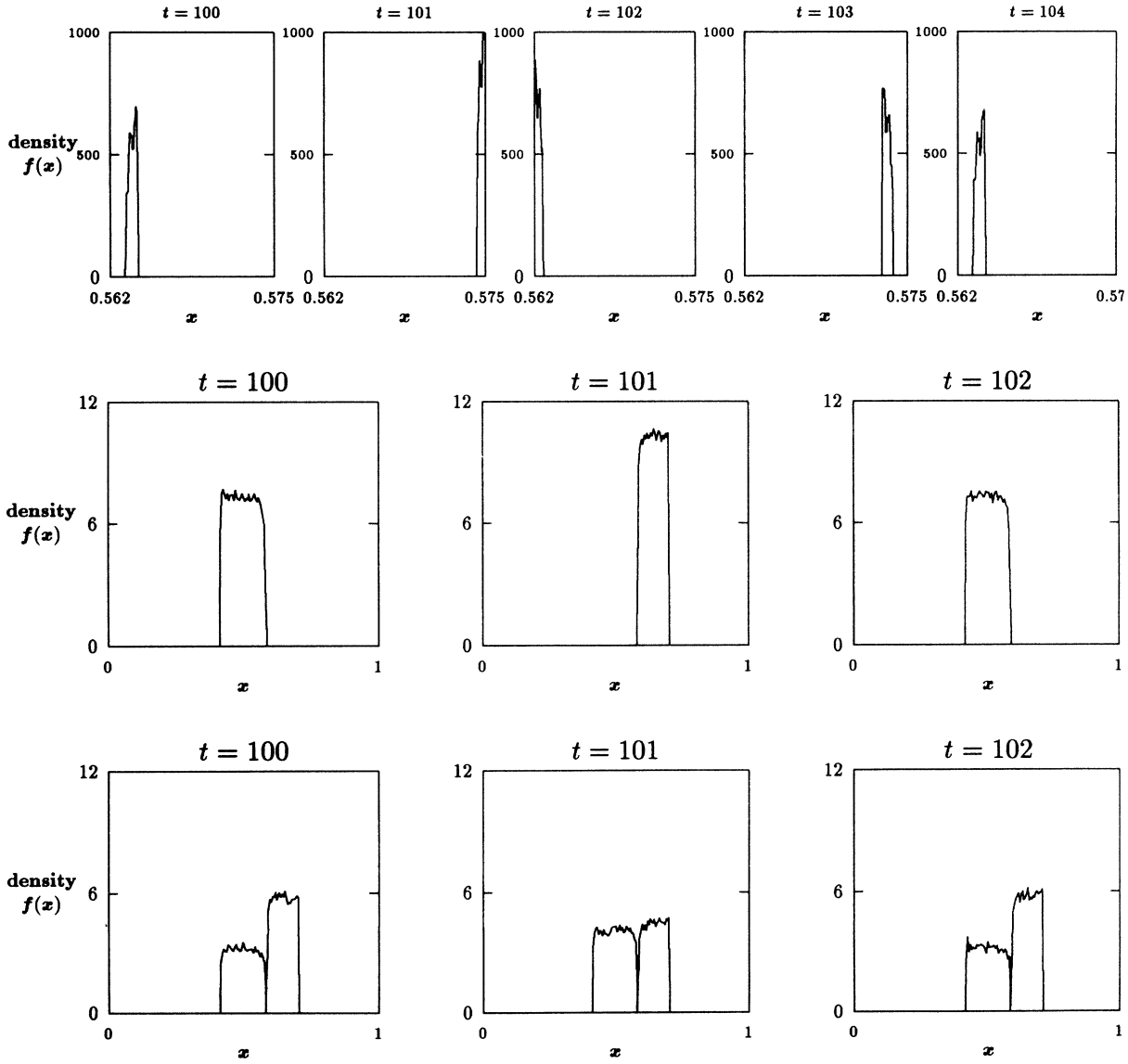

FIG. 1. Density evolution in the tent map (6): top row, when it is asymptotically periodic (AP) with period-4 ($a=1.15$) (the initial density is uniformly distributed on [0.562:0.565]); middle row, when it is AP with period-2 ($a=1.4$) (the initial density was uniform on [0.3:0.4]); bottom row, same parameters as in the middle, except the initial density is now uniform on [0:1]. This illustrates a generic property of asymptotically periodic systems: The density cycle depends sensitively on the initial ensemble density.

cally in time. A recipe for finding the r_n's is given in [24]. A rigorous proof of the asymptotic periodicity of $\mathcal{P}$ is available at these values (not in their neighborhood), and the numerics strongly indicate that the "banded-chaotic" behavior is in fact asymptotic periodicity [19].

In the next section, we given numerical evidence that statistical cycling is observed in large lattices of coupled quadratic and tent maps and that it is a signature of underlying asymptotic periodicity.

III. PHENOMENOLOGY

In this section we numerically investigate the behavior of a two-dimensional lattice of diffusively coupled maps, when the local dynamics are given by the quadratic map (9) and by the generalized tent map (6). The systems considered are Eq. (2) with $L=M=200$. The two parameters describing the evolution of the motion are r (for the quadratic map), the local slope a (for the tent map), and

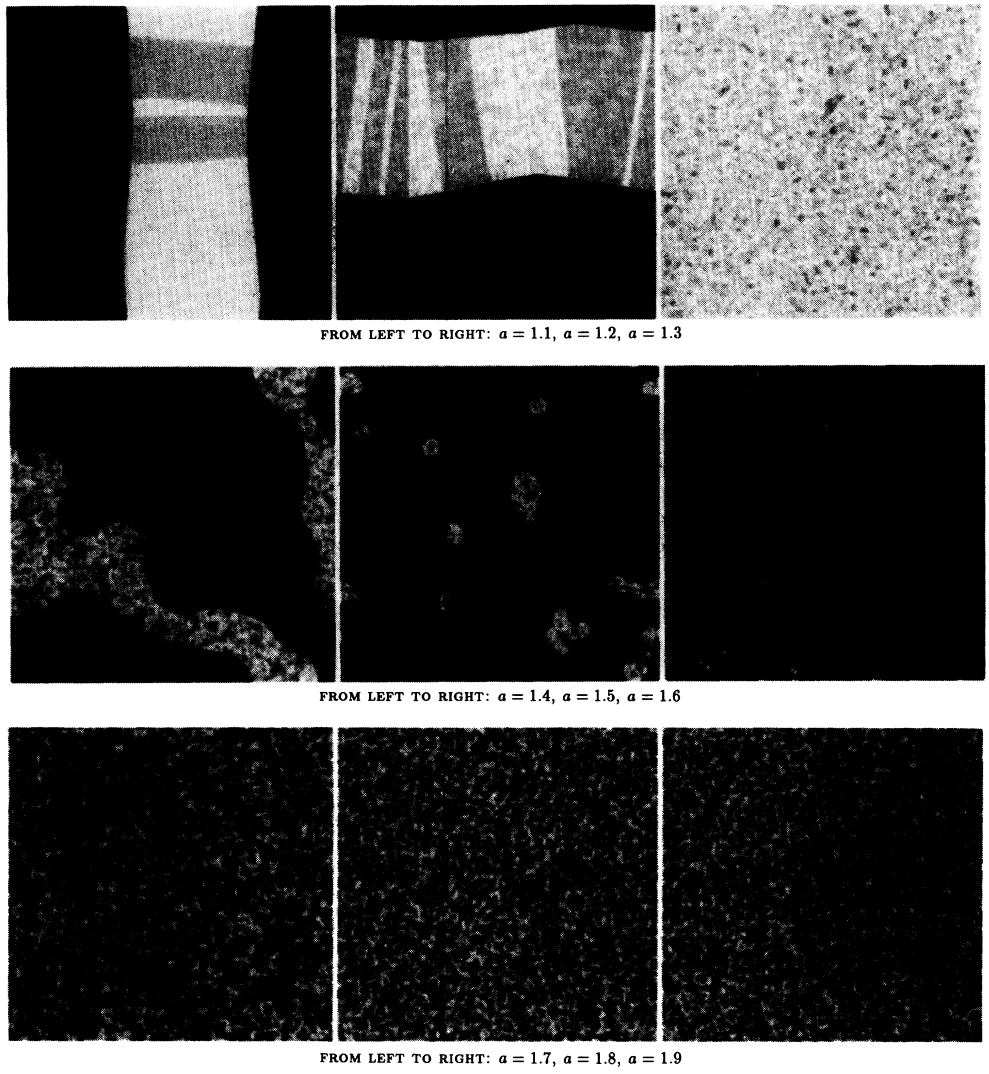

FIG. 2. Snapshots of the activity at the surface of a 200×200 lattice of diffusivity coupled tent maps when the coupling is constant ($\varepsilon=0.45$), but the local slope is increased from $a=1.1$ to 1.9. For all panels, the transient discarded is of length 10^5. The 256 grey scales range from black when $x^{i,j}=x_{\min}$ to white when $x^{i,j}=x_{\max}$, where $x_{\min}$ and $x_{\max}$ are the lower and upper bounds of the attracting subinterval of [0,1], respectively. The initial values on the lattice were in all cases given by a random number generator yielding uniform distributions on the unit interval. The transition from statistical cycling to statistical equilibrium occurs between $a=1.5$ and 1.6 for this value of the coupling. This observation is not made from the figure, but with the help of the statistical quantifiers of the motion described below (cf. Figs. 5–7). The time evolution for the $a=1.3$ case looks very much like the evolution of the three panels in Fig. 3(a) for the quadratic map. For other statistically cycling cases, the light shades of grey are mapped into darker shades and vice versa at each time step. The bottom three panel displays spatiotemporal chaos. They have reached their asymptotic state.

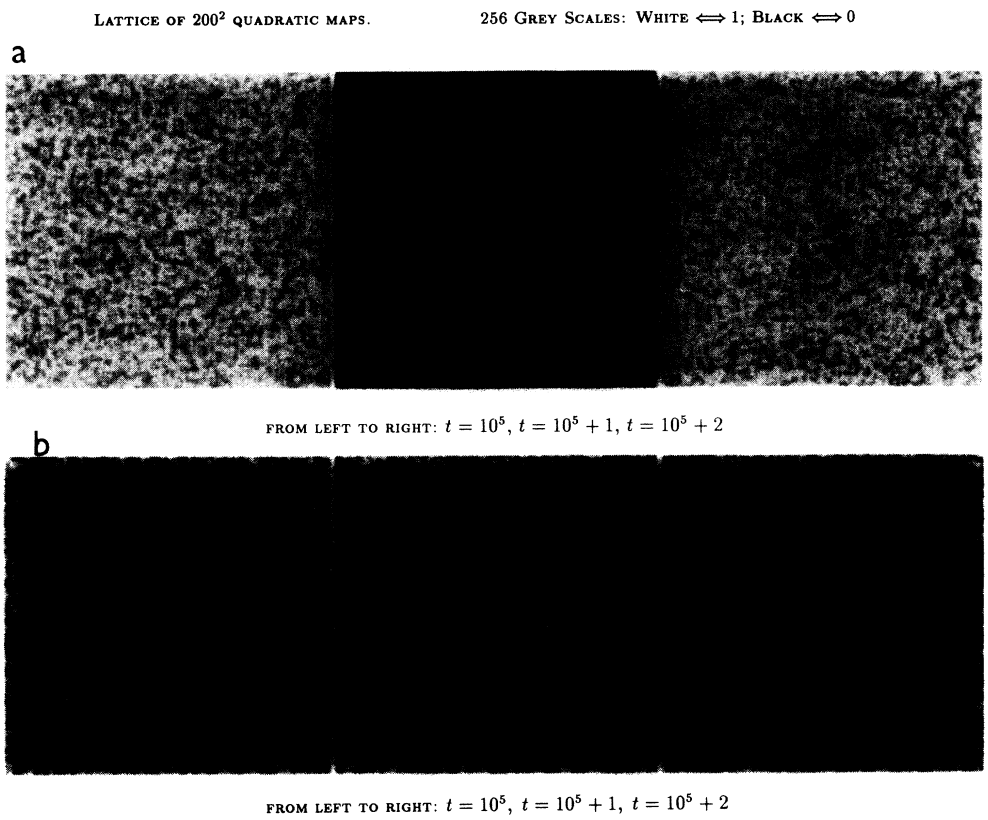

FIG. 3. The six panels display two phases of a 200×200 lattice of coupled quadratic maps with $\varepsilon = 0.45$. 10^5 transient iterations are discarded. (a) The system is statistically periodic with period-2 and $r = 3.678$. The evolution is reminiscent of that already observed in the tent map lattices with $a = 1.3$ and $\varepsilon = 0.45$. It is of interest to note that quadratic map lattices were not observed numerically to form large scale patterns in the AP region, when the initial preparations did not contain any spatial information. This is in contrast with the pattern forming behavior of the tent map lattices. (b) The system is fully turbulent and the parameter $r = 3.9$. For other parameter value, cycles of period-3 can also be observed in the lattice. In all cases, the exact asymptotic cycle depends on the initial preparation of the system, a property expected in an symptotically periodic dynamical system.

the coupling parameter ε. Two different sets of numerical experiments can therefore be carried out. The first involves changing parameters in the local nonlinearity (r or a) while keeping the coupling ε constant and the second involves changing the coupling ε while the local nonlinearity parameter remains fixed.

Figure 2 displays nine panels, each of which is a snapshot of the activity of the lattice after a transient of 10^5 iterations has been discarded. The coupling is constant in the figure and the parameter that is being changed is the slope a.

In Fig. 2 two qualitatively different types of behaviors are observed in parameter space: One is characterized by the evolution of large scale patterns from the random initial conditions; this is the clustered, or ordered, state $a = 1.1, \ldots, 1.5$ (the panel $a = 1.3$ presents an interesting limiting case for which the "cluster" covers the entire area of the lattice; different initial conditions for such parameter values evolve to the more usual large scale patterns). This pattern-forming behavior is accompanied by statistical cycling in the lattice (the term is explained in detail below). The other is characterized by the absence of such patterns; this is the spatiotemporal chaos state [9], which is described statistically by a unique invariant measure generated by almost all initial conditions. Figure 3 displays the activity of a lattice of 200×200 quadratic maps coupled diffusively. The top three panels illustrate the behavior of the lattice in the statistically cycling region, while the bottom three illustrate the fully turbulent and statistically stable regions. Note the absence of large scale patterns even in the asymptotically periodic regime, in marked contrast to the tent map lattice.

We now discuss the second set of numerical experiments which involves studying the evolution of the lattice when the slope is fixed but the coupling is varied. Figure 4 displays a transition from statistical stability to statistical cycling in the tent map CML when the slope is $a = 1.5$ as the coupling is increased from 0 to 1. When the coupling is 0, it follows from the results in [19] that the lattice will possess a unique invariant measure which will be reached for almost all initial preparation, because the local map possesses this property. For low values of the coupling, an invariant measure is also reached numerically, and this result is consistent with the analytical investigations of Keller and Künzle [2] and Gundlach and Rand [3]. When the coupling is increased (for $a = 1.5$),

there is a critical value ε_c, above which the lattice no longer reaches statistical equilibrium. Rather it reaches the "ordered" phase, characterized by cyclical statistical behavior. This statistical cycling is therefore coupling induced and it is the generalization to higher dimensions of a phenomenon described analytically in two-dimensional maps, constructed by coupling two identical maps of the interval [21]. It was shown numerically in [21] that this behavior could be expected in generic maps with quadratic maxima.

Sometimes it is a nontrivial task to decide to which state a particular panel belongs to by simply looking at the activity of the lattice. To this end, we characterize the two phases with the help of statistical quantifiers which behave qualitatively differently depending on the phase of the lattice.

A. The "collapsed density"

This time-dependent quantity is simply the density of activity on a lattice at time t. Let $\mathbf{f}(\mathbf{x}_t)$ denote the phase space density for the lattice (3), where $\mathbf{x}_t=(x_t^{0,0},\ldots,x_t^{N,N})$ is the state of the lattice. This density clearly cannot be represented graphically and it is numerically expensive to obtain when working with large lattices. We therefore approximate its "collapsed version"

$$\mathbf{f}_t^c(z)=\int\cdots\int \mathbf{f}(\mathbf{x})\prod_{i,j}\delta(x_t^{i,j}-z)dx^{i,j} \tag{11}$$

with the density f_t^c of activity across a single lattice defined implicitly by

$$\langle x_t\rangle=\frac{1}{N^2}\sum_{i,j}x_t^{i,j}f_t^c(x_t^{i,j})\ ,$$

where $\langle\ \rangle$ denotes the average of the quantity inside the angular brackets. The purpose of this reduction is to characterize the two phases of the CML efficiently and unambiguously, and f_t^c is appropriate for this task. In addition, it is easy to show that if f_t^c is stationary in time, then $\mathbf{f}$ is *almost surely* stationary, while if f_t^c cycles, $\mathbf{f}$

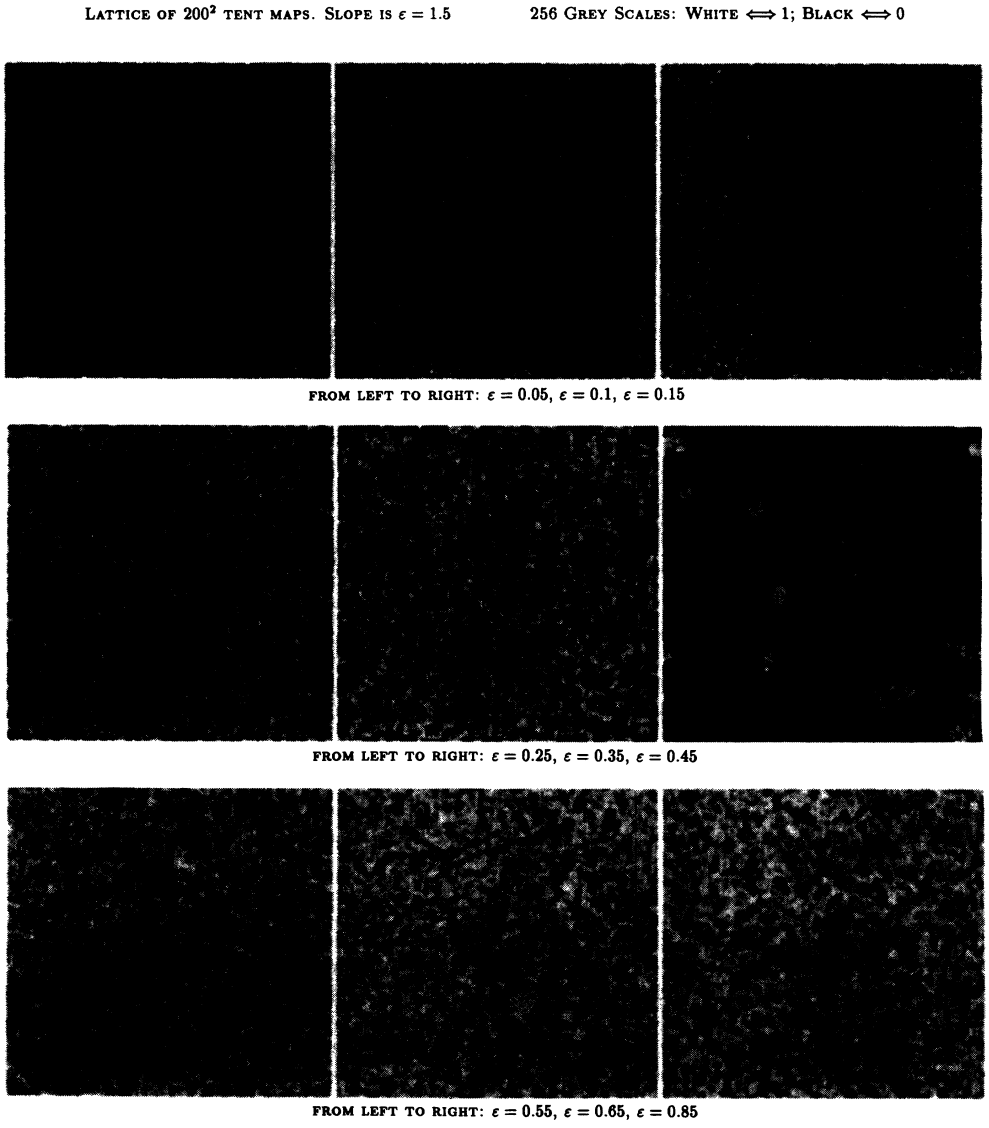

FIG. 4. Snapshots of the activity of a 200×200 lattice of tent maps with a slope of $a=1.5$. The transients discarded are of length 10^5 in each panel. At low values of the coupling, the lattice generates an invariant measure for almost all initial preparations and displays fully developed spatiotemporal chaos. At values of $\varepsilon>\varepsilon_c$, the lattice possesses an invariant measure, but it is almost never observed numerically. Instead, the phase space densities evolve to a periodic cycle which depends on the initial density. This reflects the coupling-induced asymptotic periodicity of the Perron-Frobenius operator for the lattice. The critical value of the coupling is $\varepsilon_c\simeq0.2$ when $a=1.5$. The time evolution of the lattice in the bottom three panels is similar to the "flipping" shown in Fig. 3(a).

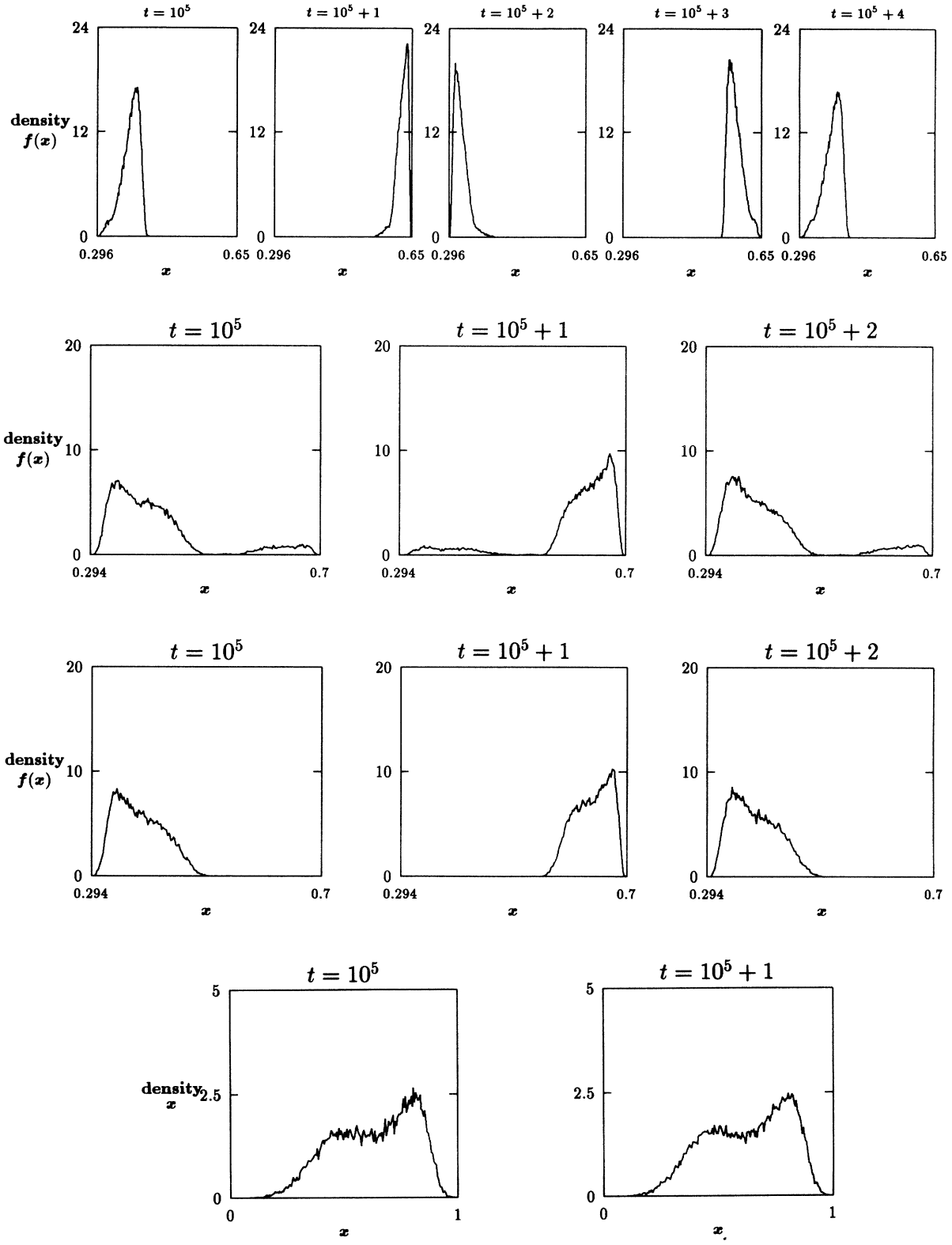

FIG. 5. The collapsed density f_i^c for A 200×200 lattice of diffusively coupled tent maps with $\varepsilon = 0.45$. The first 10^5 iterations are discarded as transients. In the top row the cycle is of period-4 and $a = 1.3$. The initial density was uniformly distributed on [0.3:0.4] (the notation $[a:b]$ denotes the closed interval between a and b). In the second row from top the cycle is of period-2, $a = 1.4$, and the initial density was uniformly distributed on [0,1]. In the third row the parameters are the same as in the second row, but with an initial density supported on [0.39:0.43]. Note, as in Fig. 1, the dependence of the asymptotic cycle on the initial density. In the bottom row the slope of the map is $a = 1.99$ and the initial density is [0,1]. This density is numerically reached for all initial densities. Here the system is "fully turbulent" or "spatiotemporally chaotic."

must cycle. By *almost surely,* we simply mean that it is possible to initialize a lattice such that the cyclical behaviors of groups of sites on the lattice (a group consisting in a number of sites not necessarily spatially close) cancel each other's cycling on average, so that f_t^c does not reflect the behavior of $\mathbf{f}$. This situation is not expected to be observed for typical preparations of finite size lattice, because it is not "robust": A slight statistical perturbation of the initial preparation will almost surely (in the space of initial densities) yield a preparation such that the groups of sites do not cancel anymore, and therefore $\mathbf{f}$ and f_t^c will both be time periodic. Therefore f_t^c gives an efficient tool for studying certain properties of $\mathbf{f}$, and its behavior is illustrated in Fig. 5.

Figure 5 displays the evolution of f_t^c when the lattice is in a period-four region, a period-2 region, and in the equilibrium (fully turbulent) regime. It is easy to show that if cycles f_t^c in time, then $\mathbf{f}(\mathbf{x}_t)$ will also. This observation is important since in Sec. IV we give conditions on a and ε which are sufficient to guarantee the cycling of $\mathbf{f}$, and interpret numerically observed cyclicity in the CML as the manifestation of a simple property of the operator governing the evolution of $\mathbf{f}$. When the cycling in the collapsed density is difficult to discern visually, studying the Boltzmann-Gibbs (BG) entropy of f_t^c highlights either stationary behavior or cycling behavior.

B. The Boltzmann-Gibbs entropy

The Boltzmann-Gibbs entropy of a system is the Boltzmann-Gibbs entropy of the phase space density which describes the ensemble statistics for the said system. In our case, the Boltzmann-Gibbs entropy for the CML is

$$H_t(\mathbf{f})=\int_{\mathbf{X}} \mathbf{f}\ln\mathbf{f}\, d\mathbf{x}_t \ , \tag{12}$$

where $\mathbf{X}$ is the phase space of the CML. This quantity was first introduced by Boltzmann [25] in a slightly different form, which assumed that the equilibrium invariant density was uniform over the phase space. Subsequent work confirmed that the definition (12) was the only (up to a multiplicative constant) possible definition of the thermodynamic entropy if the equilibrium density was the uniform density. For systems in which this is not the case, a generalization of (12), called the conditional entropy and discussed in Sec. VI, must be introduced and can be shown to satisfy the strongest forms of the second law of thermodynamics [26]. In Fig. 6 different types of entropy evolution displayed by the tent map lattices are shown. It is easy to show that the cyclical behavior of the BG entropy for the collapsed density implies cyclical behavior of the BG entropy of the phase space densities. This provides us with a powerful numerical tool with which we can probe the behavior of the thermodynamic equilibrium states of CML's.

Finally, the autocorrelation and cross correlation functions were used to confirm the statistical oscillations observed in the "ordered phase." In the tent map lattice, it is seen that the oscillations of the temporal autocorrelation function

$$\begin{aligned}\rho^{i,j}(k)&=\frac{c_k}{c_0}\ ,\\ c_k&=\frac{1}{N}\sum_{t=1}^{N-k}(x_t^{i,j}-\langle x^{i,j}\rangle)(x_{t+k}^{i,j}-\langle x^{i,j}\rangle)\ ,\end{aligned} \tag{13}$$

shown in Fig. 7, correspond to slow oscillations in the spatial cross correlation, thus reflecting the presence of large clusters of synchronized activity.

The numerical results presented in this section clearly indicate that in the CML's considered, there are two easily identifiable "phases": In one, the statistical quantifiers of the motion reach a unique equilibrium, while in the other, the same quantifiers reach a periodic cycle. These two phases reflect qualitatively different properties of the operator which evolves densities in the CML's: the Perron-Frobenius operator. A description of this operator in higher dimensions is given in the next section.

IV. PROPERTIES OF THE PERRON-FROBENIUS OPERATOR FOR CML'S

In Sec. II the Perron-Frobenius operator for the tent map and for the quadratic map was explicitly given.

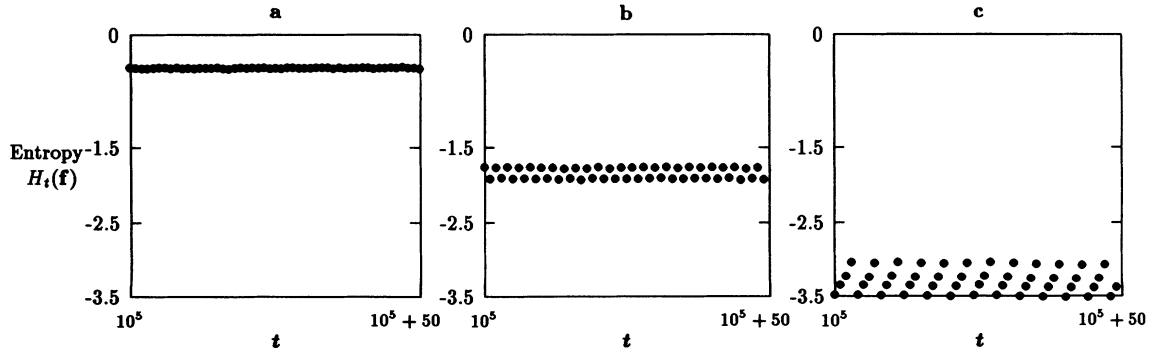

FIG. 6. The Boltzmann-Gibbs entropy for the collapsed density of a lattice of 200×200 diffusively coupled tent maps. $\varepsilon=0.45$ in all three panels. (a) $a=1.99$, the CML is spatiotemporally chaotic. (b) $a=1.4$, the CML is AP period-2. (c) $a=1.3$, the CML is period-4. The initial density was uniformly distributed on [0,1] for all three panels.

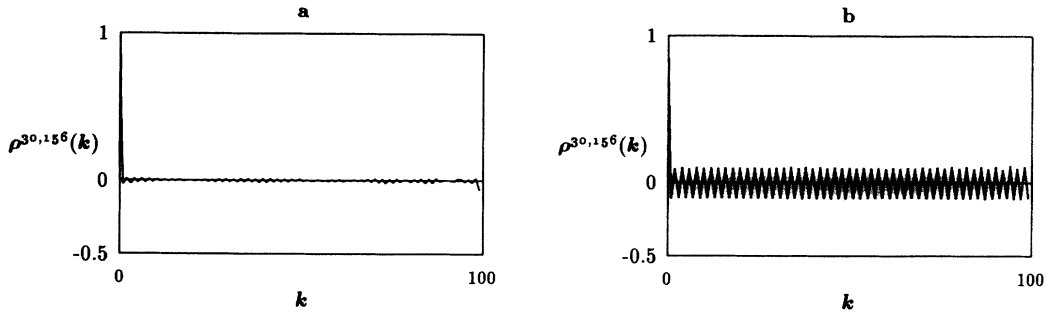

FIG. 7. Temporal autocorrelation function (13) of the activity at site (36,156) (chosen for no particular reason) on a lattice of tent maps diffusively coupled with $\varepsilon=0.45$ with the first 10^5 iterations discarded as transients and the initial activity of the lattice uniformly distributed on [0,1]. (a) The lattice is fully turbulent with $a=1.99$. (b) The slope is $a=1.4$ and the cyclical behavior of $\rho^{36,156}(k)$ reflects the statistical cycling in the lattice [k denotes time in this expression, as in (13)].

Since we are interested in the dynamics of CML's, we must discuss the dynamics of the Perron-Frobenius operator acting on $\mathcal{N}$-dimensional densities if there are $\mathcal{N}$ elements in the lattice. Explicit expressions are not very useful in this case; rather one can obtain some insight into the dynamics of the system by studying the spectral properties of the PF operator. The kinds of properties we seek are, for example, the existence of a complete set of eigenfunctions in terms of which densities can be expressed and, more importantly, conditions on the parameters of the CML which guarantee a "cyclical" spectral decomposition, which implies the statistical behavior defined in (5) and observed numerically in Sec. III. To do so, a few mathematical definitions are needed.

Definitions

Let the set of non-negative elements of L^1 be denoted

$$L^1_+ = \{f \in L^1 : f(x) \geq 0 \text{ almost everywhere}\}$$

and the set of densities by

$$D = \{f \in L^1_+ : \|f\|_{L^1} = 1\} ,$$

where $\| \|_{L^1}$ denotes the L^1 norm

$$\|f\|_{L^1} \equiv \int_{\mathbb{X}} |f(x)| dx = \int_{\mathbb{X}} f(x) dx$$

for densities. The bounded variation norm, which we will use later, is denoted by $\| \|_{BV}$ and defined by

$$\|f\|_{BV} = \|f\|_{L^1} + \|\nabla_d f\|_{L^1} \equiv \|f\|_{L^1} + \mathcal{V}(f) ,$$

where $\mathcal{V}(f)$ denotes the variation of f and the ∇_d operator is defined in the distributional sense: In dimension $\mathcal{N}$, it is a vector-valued measure $(\text{div}_1(f), \text{div}_2(f), \ldots, \text{div}_{\mathcal{N}}(f))$, where f is a real-valued function defined on a open subset $\mathbb{X} \subset \mathbb{R}^{\mathcal{N}}$ and such that there are signed measures $\mu_1, \ldots, \mu_{\mathcal{N}}$ and test functions $\psi \in \mathcal{C}(\mathbb{X})$

$$\int_{\mathbb{R}} f \, \text{div}_i(\psi) d\mu_L^{\mathbb{R}} = \int_{\mathbb{R}} \psi \, d\mu_i , \quad i = 1, \ldots, \mathcal{N} ,$$

where $\mathcal{C}(\mathbb{X})$ is the space of functions from $\mathbb{X}$ to $\mathbb{X}$ having compact support, $\text{div}_i(\psi) = \partial\psi/\partial x_i$, and $\mu_L^{\mathbb{R}}$ is the Lebesgue measure in $\mathbb{R}$ (cf. [27,2] for details). With these preliminaries, the definition of variation of f is [27]

$$\mathcal{V}(f) = \|\nabla_d f\|_{L^1} = \sup \left\{ \int_{\mathbb{X}} f \, \text{div}(\mu) d\mu_L^{\mathbb{X}} : \psi = (\psi_1, \ldots, \psi_N) \in \mathcal{C}(\mathbb{X}) \right\} .$$

The result we present follows from the application of a theorem of Ionescu Tulcea and Marinescu [28] to the Perron-Frobenius operator, considered as an operator acting on functions of bounded variation. In order for this theorem to apply, we need to verify that the Perron-Frobenius operator satisfies four conditions, which are discussed in [15]. Góra and Boyarski show in Sec. III of [15] that three of these conditions are essentially satisfied by $\mathcal{P}_\Phi$ irrespective of Φ (unless $\mathbb{X}$ possesses pathological properties, which we need not worry about here), since they depend on the operator norm of $\mathcal{P}_\Phi$ and on basic properties of the function space $BV(\mathbb{X})$ in which it operates. The last condition to be satisfied in order for Ionescu Tulcea and Marinescu's theorem to apply is (a) that there exist constants $Q > 0$ and $0 < q < 1$ such that

$$\|\mathcal{P}_\Phi f\|_{BV} \leq q\|f\|_{BV} + Q\|f\|_{L^1} \quad \text{for } f \in BV(\mathbb{X}) ,$$

where $BV(\mathbb{X})$ is the Banach space of real-valued functions defined on $\mathbb{X}$ with finite (i.e., bounded) variation ([27], Remark 1.12). When considering probability densities, the condition (a) can be replaced by the following: (a') there exist constants $\Omega > 0$ and $0 < \omega < 1$ such that

$$\mathcal{V}(\mathcal{P}_\Phi f) \leq \omega \mathcal{V}(f) + \Omega \quad \text{for } f \in D . \tag{14}$$

If condition (a') holds (as well as the three other ones, always satisfied in practice, and discussed rigorously in [15]), then the Perron-Frobenius operator induced by the CML Φ and defined by (4) is asymptotically periodic: The density evolution is as described in Remark 1 and (1) $\mathcal{P}_\Phi$ has a finite number of eigenvalues of modulus 1: $\kappa_1, \ldots, \kappa_l$. They are the roots of unity and

$$\mathcal{P}_\Phi = \sum_{i=1}^{l} \kappa_i \mathcal{P}_i + T \ , \tag{15}$$

where $\mathcal{P}_i$: $BV(\mathbf{X}) \to BV(\mathbf{X})$ are linear projections with finite-dimensional range. (2) $\mathcal{P}_i^2 = \mathcal{P}_i$, $\mathcal{P}_i \mathcal{P}_j = 0$ $(i \neq j)$, and $\mathcal{P}_i T = T \mathcal{P}_i = 0$, $1 \leq i,j \leq l$. (3) For any $f \in D$, $\| T^n f \|_{L^1} \to 0$, as $n \to \infty$ (T is a "transient operator").

As a direct consequence of this representation for the Perron-Frobenius operator, it is possible to show that there are probability densities $g_1, \ldots, g_r$ of bounded variation, a measurable partition $C_1, \ldots, C_r$, and a permutation α of $\{1, \ldots, r\}$ such that (1') for every $f \in D$

$$\left[\sum_{i-1}^{l} \mathcal{P}_i \right](f) = \sum_{k=1}^{r} \int_{C_k} f \, d\mu_L^M g_k \ ,$$

where again $d\mu_L^M$ denotes the Lebesgue measure in $\mathbb{R}^M$; (2') $\mathcal{P} g_k = g_{\alpha(k)}$, $k = 1, \ldots, r$; and (3') $\int_{C_i} g_k \, d\mu_L^M = \delta_{i,k}$, where δ is the Kronecker symbol.

In other words the evolution of densities is as described in Remark 1 for asymptotically periodic systems. The proof of the connection between the spectral representation [(1),(2),(3)] of the Perron Frobenius operator and the cyclical density evolution [(1'),(2'),(3')] is given in [29].

V. APPLICATION TO LATTICES OF TENT MAPS

In this section we use the ideas developed in the previous one to examine the spectral properties of the Perron-Frobenius operator as the parameters a and ε are varied and give sufficient conditions for asymptotic periodicity in a square lattice with N^2 elements as a function of a, ε, and lattice size. Our condition is obtained by verifying in which regions of parameter space inequality (14) is satisfied: The quantity $\mathcal{V}(\mathcal{P}_\Phi f)$ is estimated and the constant ω in (14) is determined. It is seen to be greater than 0 all the time, and setting $\omega < 1$ therefore yields the desired sufficient condition.

It is useful to visualize the CML Φ defined in (2) as a matrix acting on a state vector $\mathbf{x}_t$: $\Phi(\mathbf{x}_t) = \mathbf{x}_{t+1}$, where

$$\Phi(\mathbf{x}_t) = \begin{bmatrix} (1-\varepsilon)S(x_t^1) & \frac{\varepsilon}{4}S(x_t^2) & 0 & \frac{\varepsilon}{4}S(x_t^N) & 0\frac{\varepsilon}{4}S(x_t^{N^2-N}) & 0 & \frac{\varepsilon}{4}S(x_t^{N^2}) \\ \frac{\varepsilon}{4}S(x_t^1) & (1-\varepsilon)S(x_t^2) & \frac{\varepsilon}{4}S(x_t^3) & 0 & \frac{\varepsilon}{4}S(x_t^{N+1}) & 0\ \frac{\varepsilon}{4}S(x_t^{N^2-N+1}) & 0 \\ \ddots & \ddots & \ddots & \ddots & \ddots & \ddots & \ddots \\ \frac{\varepsilon}{4}S(x_t^1) & 0 & \frac{\varepsilon}{4}S(x_t^N) & 0 & \frac{\varepsilon}{4}S(x_t^{N^2-N}) & 0\ \frac{\varepsilon}{4}S(x_t^{N^2-1}) & (1-\varepsilon)S(x_t^{N^2}) \end{bmatrix} \tag{16}$$

with

$$\mathbf{x}_t \equiv \begin{bmatrix} x_t^2 \\ x_t^2 \\ \vdots \\ x_t^{N^2} \end{bmatrix} .$$

As an aside, this representation of the lattice activity highlights the fact that local coupling in two dimensions is equivalent to long range coupling in one. More importantly, it allows us to calculate the Euclidean matrix norm of Φ readily, and we need this norm to apply some results of [15] to set upper bounds on $\mathcal{V}(\mathcal{P}_\Phi f)$.

Statement of result

The CML (2) with nonlinearity (6) (and N^2 elements) induces a Perron Frobenius operator $\mathcal{P}_\Phi$ which admits a representation of the form (15) [which implies (1',2',3')] if

$$\prod_{j=1}^{N^2} \lambda_j^2 [1+\sigma] < 1 \ , \tag{17}$$

where σ is given explicitly below Eq. (20), and where the λ_j's are the eigenvalues of $\mathcal{J}(\Phi)$, the absolute value of the derivative matrix of Φ:

$$\mathcal{J}(\Phi) = \begin{bmatrix} (1-\varepsilon)a & \frac{\varepsilon}{4}a & 0 & \frac{\varepsilon}{4}a & 0 & \frac{\varepsilon}{4}a & 0 & \frac{\varepsilon}{4}a \\ \frac{\varepsilon}{4}a & (1-\varepsilon)a & \frac{\varepsilon}{4}a & 0 & \frac{\varepsilon}{4}a & 0 & \frac{\varepsilon}{4}a & 0 \\ & & & & \ddots & & & \\ \frac{\varepsilon}{4}a & 0 & \frac{\varepsilon}{4}a & 0 & 0\frac{\varepsilon}{4}a & 0 & \frac{\varepsilon}{4}a & (1-\varepsilon)a \end{bmatrix} .$$

In order to obtain inequality (14), we calculate bounds on $\mathcal{V}(\mathcal{P}_\Phi f)$:

$$\begin{aligned}\mathcal{V}(\mathcal{P}_\Phi f)&=\mathcal{V}\left[\sum_{i=1}^{m}\frac{f(\Phi_i^{-1}(x))}{\det\mathcal{J}(\Phi_i^{-1}(x))}\chi_{\Phi_i(A_i)}(x)\right]\\&\le\sum_{i=1}^{m}\mathcal{V}\left[\frac{f(\Phi_i^{-1}(x))}{\det\mathcal{J}(\Phi_i^{-1}(x))}\chi_{\Phi_i(A_i)}(x)\right]\\&=\det\mathcal{J}(\Phi^{-1})^{-1}\sum_{i=1}^{m}\mathcal{V}(f(\Phi_i^{-1}(x))\chi_{\Phi_i(A_i)}(x)),\quad m=2^{N^2},\end{aligned}\tag{18}$$

where the substitution $\mathcal{J}(\Phi_i^{-1}(x))\to\mathcal{J}(\Phi^{-1})$ follows from the fact that the determinant $\det\mathcal{J}(\Phi_i^{-1}(x))$ can always be shown, by an appropriate multiplication of the columns of $\mathcal{J}(\Phi_i^{-1}(x))$ by either 1 or -1, to be equal to the determinant of the simpler matrix $\mathcal{J}(\Phi^{-1})$ [this is a straightforward consequence of the basic properties of determinants (namely, *general property 39,* p. 25 of [30])]. $\mathcal{J}(\Phi)$ is real and symmetric, and therefore it is diagonalizable and its determinant is the product

$$\det\mathcal{J}(\Phi)=\prod_{j=1}^{N^2}\lambda_j=\det\mathcal{J}(\Phi^{-1})^{-1},\tag{19}$$

where the λ_j's are its eigenvalues.

Using the proof of Lemma 4 and the example of Sec. II in [15], and Example 1.4 in [27], the quantity $\mathcal{V}(f(\Phi_i^{-1}(x))\chi_{\Phi_i(A_i)}(x))$ is seen to satisfy

$$\begin{aligned}\mathcal{V}(f(\Phi_i^{-1}(x))\chi_{\Phi_i(A_i)}(x))&\le\mathcal{V}(f(\Phi_i^{-1}(x)))+\int_{\mathbb{R}^{N^2}}\|f(\Phi_i^{-1}(x))\nabla_d\chi_{\Phi_i(A_i)}\|_{L^1}d\mu_L^{N^2}\\&=\mathcal{V}(f(\Phi_i^{-1}(x)))+\int_{\partial\Phi_i(A_i)}|f(\Phi_i^{-1}(x))|d\mu_L^{N^2-1}\\&\le\mathcal{V}(f(\Phi_i^{-1}(x)))+\sigma\{\mathcal{V}(f(\Phi_i^{-1}(x)))+\mathcal{H}\}\\&=\mathcal{V}(f(\Phi_i^{-1}(x)))[1+\sigma]+\sigma\mathcal{H}\end{aligned}\tag{20}$$

with $\mathcal{H}>0$ and σ defined to be

$$\sigma=\left[\frac{N^2[1+(N^2-2)\cos\theta]}{1-\cos\theta}\right]^{-1/2},$$

$$\theta=\tan^{-1}\left[\frac{4(1-\varepsilon)[\varepsilon^2-16(1-\varepsilon)^2]}{\varepsilon[\varepsilon^2+16(1-\varepsilon)^2]}\right].$$

Both σ and θ depend on the geometry of the sets A_i. The formulas given here hold if the faces of the A_i meet at right angles, which is clearly the case since S is the tent map. Their detailed derivation is rather lengthy and will be presented elsewhere. Using (19), and summing the terms such as (20) in (18), we reach the inequality

$$\mathcal{V}(\mathcal{P}_\Phi f)\le\left[\prod_{i=1}^{N^2}\lambda_i\right]^2[1+\sigma]\mathcal{V}(f)+2^{N^2}\sigma\mathcal{H}.\tag{21}$$

[To obtain the factor $2^{N^2}\sigma\mathcal{H}$ we have used the fact that for a square lattice of tent maps, the eigenvalues are bounded above by the maximum slope, which in our case is $a=2$; cf. Eqs. (22) and (23).] Comparing (21) with (14), identifying ω in (14) with the coefficient of $\mathcal{V}(f)$ above, and letting $\Omega=2^{N^2}\sigma\mathcal{H}$ we immediately obtain condition (17).

We can explicitly evaluate this condition for a square lattice of tent maps because the eigenvalues can be obtained exactly: $\mathcal{J}(\Phi)$ is a circulant matrix and it is well known that the eigenvalues of such matrices can be computed [31]. In our case,

$$\lambda_j=(1-\varepsilon)a+a\varepsilon\left[\cos\left[\frac{\pi j}{N}(1-1/N)\right]\times\cos\left[\frac{\pi j}{N}(1+1/N)\right]\right]\tag{22}$$

$$\simeq(1-\varepsilon)a+a\varepsilon\cos^2\left[\frac{\pi j}{N}\right],\quad j=0,1,\ldots,N^2-1\tag{23}$$

when N is large.

Similar conditions can be obtained for rings of diffusivity coupled piecewise linear maps. Condition (17) will still hold, the transformation matrix Φ will now be tridiagonal, and if there are N elements in the ring with periodic boundary conditions, the eigenvalues of $\mathcal{J}(\Phi)$ for the ring are

$$\lambda_j=(1-\varepsilon)a+a\varepsilon\cos\left[\frac{2\pi j}{N}\right],\quad j=0,\ldots,N-1.\tag{24}$$

It should be noted that different coupling schemes can be studied using this formalism (as long as the same coupling is applied to all the elements of the lattice). The key to the applicability of the method lies in choosing systems

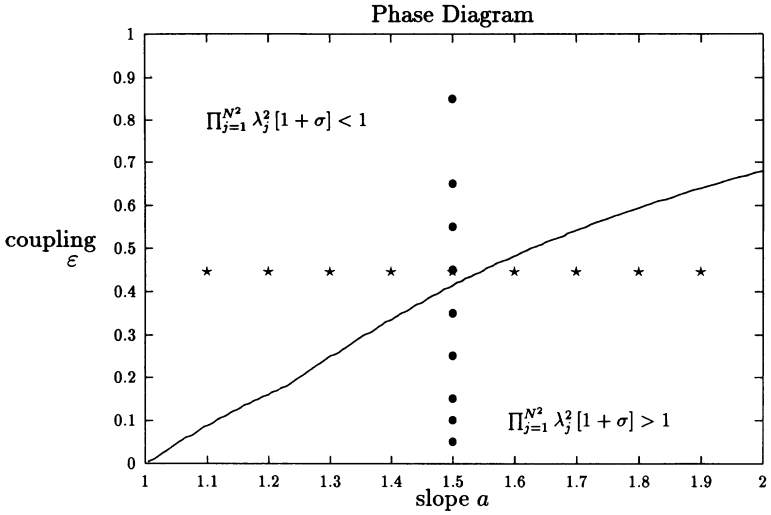

FIG. 8. The criterion (17) plotted for a lattice of 200×200 diffusively coupled tent maps. The line indicates the values of a and ε at which the left hand side of (17) equals one. In the upper left part, the criterion (17) is satisfied and the Perron Frobenius operator induced by the lattice of tent maps is asymptotically periodic. The stars indicate the positions in the (a,ε) plane of the nine panels of Fig. 2. The full circles indicate the positions of the nine panels of Fig. 4.

which have periodic boundary conditions. If this is not the case, the condition (17) holds, but the eigenvalues cannot be evaluated explicitly as easily as when the matrix Φ is circular, although special architectures are amenable to analytic investigations. Applying the criterion (17) to the 200×200 lattice which is investigated numerically in Sec. II yields Fig. 8.

VI. DISCUSSION

It is clear that the sufficient condition (17) does not give the exact locations of the numerically phase transitions discussed in Sec. III, although the phase diagram predicts the phase transitions with an accuracy of about 5% in certain regions of parameter space. The approach described here is promising because it is general: It only makes use of basic results of the theory of linear operators and it is feasible that inequalities such as (14) will be satisfied by CML's which are not expanding everywhere, although the algebra for nonpiecewise linear maps has not been tackled yet. In addition, condition (17) will hold for any piecewise linear CML which can be represented by a real symmetric matrix Φ acting on a state vector $\mathbf{x}_t$. Despite its lack of quantitative precision, it allows us to understand the cycling discussed in Sec. III as a manifestation of an interesting dynamical property of the Perron-Frobenius operator for the CML: asymptotic periodicity. This has interesting consequences for the construction of nonequilibrium statistical mechanics for these systems.

The first consequence is that ensemble statistics will depend on the initial ensemble in a sensitive way [this sensitivity is due to the dependence of the Γ_i's of Eq. (5) on the initial density] when the Perron-Frobenius operator satisfies inequality (14). In addition, in this case, even if the existence and uniqueness of an invariant measure can be proven, this measure will almost never be the relevant natural measure because it will almost never be associated with the behavior of an ensemble of systems.

The second consequence is that the thermodynamic entropy for the CML displaying asymptotic periodicity is not the Boltzmann-Gibbs entropy. Rather it is the conditional entropy with respect to the density of the invariant measure $H(\mathbf{f}|\mathbf{f}^*)$:

$$H(\mathbf{f}|\mathbf{f}^*) = -\int_{\mathbf{x}} \mathbf{f} \ln\left[\frac{\mathbf{f}}{\mathbf{f}^*}\right] d\mathbf{x} , \tag{25}$$

where $\mathbf{f}^*$ is the density of the invariant measure. This definition arises from the observation that the thermodynamic entropy is an isolated system should increase as it relaxes to equilibrium. It can be shown that H is the only possible definition of entropy which satisfies all the requirements that such an extensive quantity should meet. This illustrates the fact that in general dissipative spatially extended dynamical systems, the spontaneous ordering (reflected here by the appearance of large scale patterns) is consistent with the evolution of the entropy to a maximum.

It should be noted that the application of the Ionescu Tulcea–Marinescu theorem should yield information on the spectral properties of the transfer operators describing the evolution of measures μ_t induced by cellular automata schemes. In this last case, however, the discrete nature of the phase space precludes a consideration of absolutely continuous measures (and their densities). Instead, the supports of the measures are now generalized functions and the Perron-Frobenius operator acting on measures must be considered. The measure spaces associated with such measures can still be endowed with the bounded variation norm, and inequalities concerning the evolution of $\|f_t\|_{BV}$ under the action of the Perron-Frobenius operator can be obtained, yielding conditions on the parameters such that the inequality above (14) holds.

VII. SUMMARY

We have numerically explored a class of nonequilibrium phase transitions in finite-dimensional coupled map lattices of tent maps and quadratic maps. It is shown that these systems possess two "phases": One can be described as being spatiotemporally chaotic, and the statistical quantifiers in this case can be computed with respect

to a unique absolutely continuous invariant measure. The other is characterized by a cyclical evolution of the phase space densities. The transitions from one phase to the other can occur as a result of changing the parameter in the local nonlinearity or as a result of increasing the interelement coupling.

The spectral properties of the Perron-Frobenius operator for large CML's are examined generically to account for these phase transitions. Specifically, we give conditions on the slope of the tent map and on the strength of the coupling which guarantee a representation of the Perron-Frobenius operator implying that at equilibrium, phase space densities cycle periodically. Changes in the spectral properties of the Perron-Frobenius operator as parameters are varied are shown to be consistent with the numerical observations of different phases.

ACKNOWLEDGMENTS

The authors would like to acknowledge very useful discussions with Professor Boyarski and Professor Góra of Concordia University, in Montréal. They also wish to thank the Fonds pour la Formation des Chercheurs et l'Avancement de la Recherche for support to J.L. and the Natural Sciences and Engineering Research Council of Canada, NATO, and the Alexander von Humboldt Stiftung for support to M.C.M.

[1] L. A. Bunimovich and Ya G. Sinai, Nonlinearity **1**, 491 (1988).
[2] G. Keller and M. Künzle, Ergod. Theor. Dyn. Syst. (to be published).
[3] V. M. Gundlach and D. A. Rand, Nonlinearity **6**, 165 (1993).
[4] J. Guckenheimer and P. Holmes, *Nonlinear Oscillations, Dynamical Systems and Bifurcations of Vector Fields,* Applied Mathematical Sciences Vol. 42 (Springer-Verlag, Berlin, 1983).
[5] J. Miller and D. A. Huse, Phys. Rev. E **48**, 2528 (1993).
[6] C. Beck and F. Schlögl, *Thermodynamics of Chaotic Systems* (Cambridge University Press, Cambridge, 1993).
[7] H. Chaté and P. Manneville, Prog. Theor. Phys. **87**, 1 (1992).
[8] J. A. C. Gallas, P. Grassberger, H. J. Hermann, and P. Ueberholz, Physica A **180**, 19 (1992).
[9] K. Kaneko, Physica D **34**, 1 (1989).
[10] Y. Pomeua, J. Stat. Phys. **70**, 1379 (1993).
[11] S. Puri, R. C. Desay, and R. Kapral, Physica D **50**, 207 (1991).
[12] K. Kaneko, Chaos **2**, 279 (1993).
[13] D. Ruelle, in *Encyclopedia of Mathematics and its Applications* (Addison-Wesley, New York, 1978).
[14] V. M. Gundlach and D. A. Rand, Nonlinearity **6**, 201 (1993).
[15] P. Gorá and A. Boyarski, Isr. J. Math. **67**, 272 (1989).
[16] H. Chaté and P. Manneville, Phys. Rev. Lett. **58**, 112 (1987).
[17] A. Lasota and M. C. Mackey, *Probabilistic Properties of Deterministic Systems* (Cambridge University Press, Cambridge, 1985).
[18] P. Szépfalusy and T. Tél, Phys. Rev. A **34**, 2520 (1986).
[19] N. Provatas and M. C. Mackey, Physica D **53**, 295 (1991).
[20] T. Yoshida, H. Mori, and H. Shigematsu, J. Stat. Phys. **31**, 279 (1983).
[21] J. Losson and M. C. Mackey, Physica D **72**, 324 (1994).
[22] M. V. Jakobson, Commun. Math. Phys. **81**, 39 (1981).
[23] E. N. Lorenz, N. Y. Acad. Sci. **357**, 282 (1980).
[24] S. Grossman and S. Thomae, J. Stat. Phys. **26**, 481 (1981).
[25] C. Grandy, *Foundations of Statistical Mechanics* (Reidel, Dordrecht, 1988).
[26] M. C. Mackey, *Time's Arrow: The Origin of Thermodynamic Behavior* (Springer-Verlag, Berlin, 1992).
[27] E. Giusti, *Minimal Surfaces and Functions of Bounded Variation* (Birkhauser, Berlin, 1984).
[28] C. T. Ionescu Tulcea and G. Marinescu, Ann. Math. **52**, 140 (1950).
[29] M. Rychlik, Stud. Math. **76**, 69 (1983).
[30] T. Muir, *A Treatise on the Theory of Determinants* (Dover, New York, 1960).
[31] G. Kowalewski, *Determinanten Theorie* (Chelsea, New York, 1948).

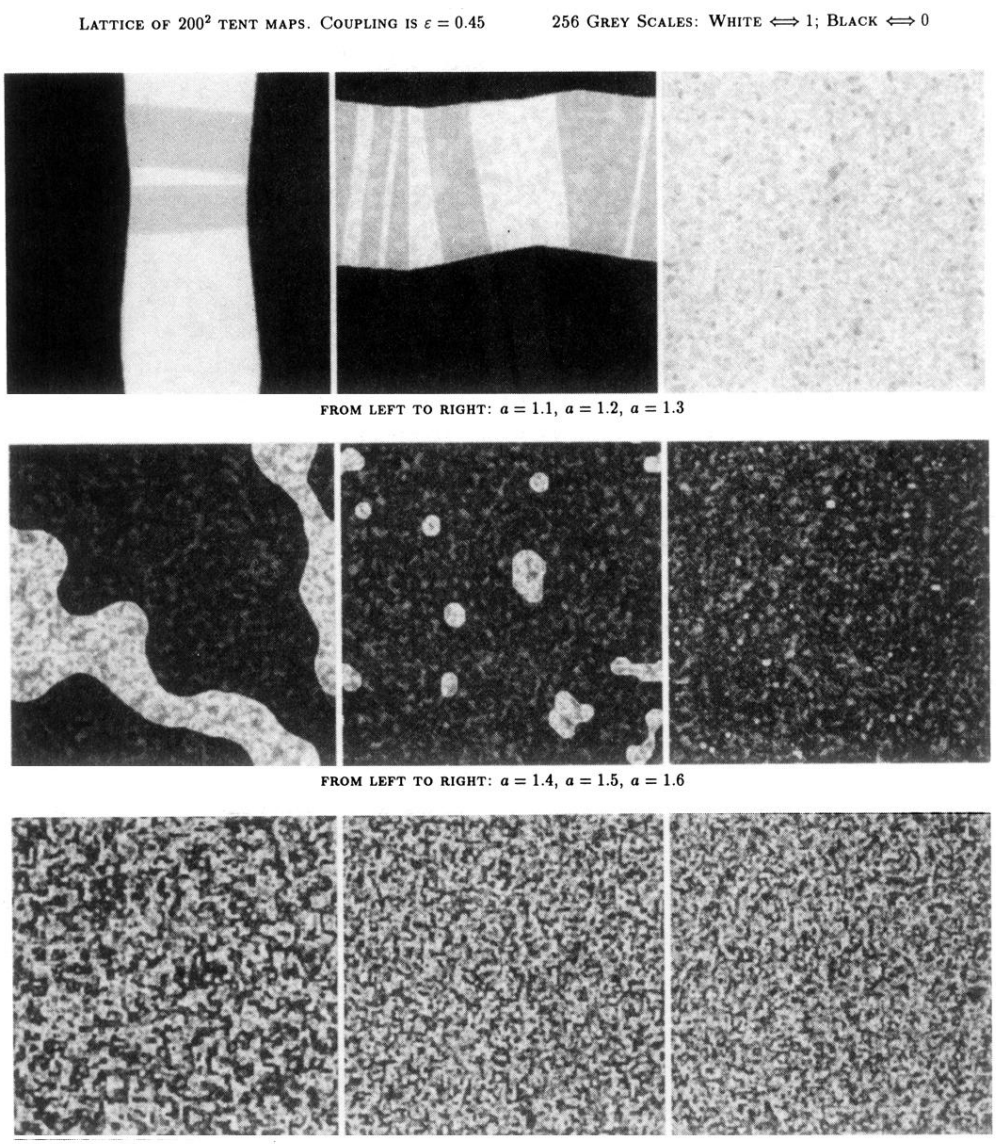

FIG. 2. Snapshots of the activity at the surface of a 200×200 lattice of diffusivity coupled tent maps when the coupling is constant ($\varepsilon = 0.45$), but the local slope is increased from $a = 1.1$ to 1.9. For all panels, the transient discarded is of length 10^5. The 256 grey scales range from black when $x^{i,j} = x_{\min}$ to white when $x^{i,j} = x_{\max}$, where $x_{\min}$ and $x_{\max}$ are the lower and upper bounds of the attracting subinterval of [0,1], respectively. The initial values on the lattice were in all cases given by a random number generator yielding uniform distributions on the unit interval. The transition from statistical cycling to statistical equilibrium occurs between $a = 1.5$ and 1.6 for this value of the coupling. This observation is not made from the figure, but with the help of the statistical quantifiers of the motion described below (cf. Figs. 5–7). The time evolution for the $a = 1.3$ case looks very much like the evolution of the three panels in Fig. 3(a) for the quadratic map. For other statistically cycling cases, the light shades of grey are mapped into darker shades and vice versa at each time step. The bottom three panel displays spatiotemporal chaos. They have reached their asymptotic state.

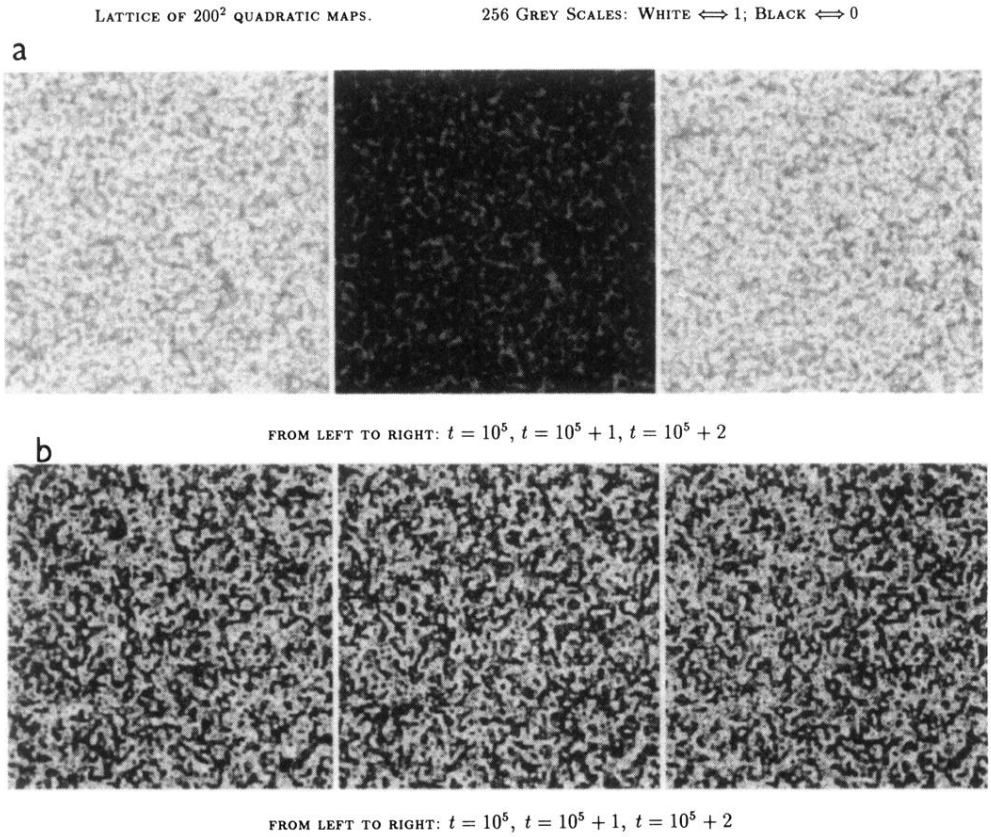

FIG. 3. The six panels display two phases of a 200×200 lattice of coupled quadratic maps with $\varepsilon = 0.45$. 10^5 transient iterations are discarded. (a) The system is statistically periodic with period-2 and $r = 3.678$. The evolution is reminiscent of that already observed in the tent map lattices with $a = 1.3$ and $\varepsilon = 0.45$. It is of interest to note that quadratic map lattices were not observed numerically to form large scale patterns in the AP region, when the initial preparations did not contain any spatial information. This is in contrast with the pattern forming behavior of the tent map lattices. (b) The system is fully turbulent and the parameter $r = 3.9$. For other parameter value, cycles of period-3 can also be observed in the lattice. In all cases, the exact asymptotic cycle depends on the initial preparation of the system, a property expected in an symptotically periodic dynamical system.

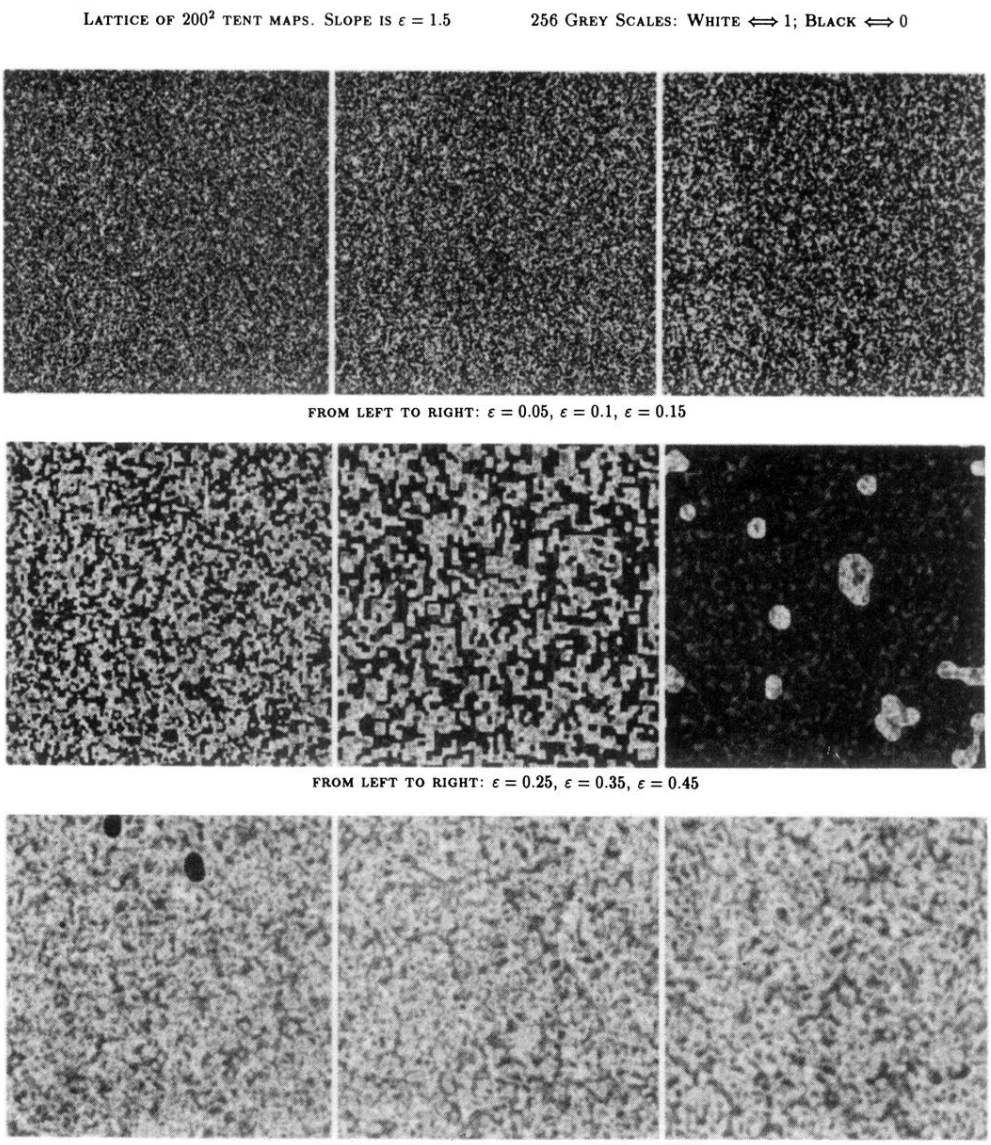

FIG. 4. Snapshots of the activity of a 200×200 lattice of tent maps with a slope of $a = 1.5$. The transients discarded are of length 10^5 in each panel. At low values of the coupling, the lattice generates an invariant measure for almost all initial preparations and displays fully developed spatiotemporal chaos. At values of $\varepsilon > \varepsilon_c$, the lattice possesses an invariant measure, but it is almost never observed numerically. Instead, the phase space densities evolve to a periodic cycle which depends on the initial density. This reflects the coupling-induced asymptotic periodicity of the Perron-Frobenius operator for the lattice. The critical value of the coupling is $\varepsilon_c \simeq 0.2$ when $a = 1.5$. The time evolution of the lattice in the bottom three panels is similar to the "flipping" shown in Fig. 3(a).